The (2+1)D Ising model on a triangular lattice

1986 J. Phys. A: Math. Gen. 19 423

(http://iopscience.iop.org/0305-4470/19/3/023)

J. Phys. A: Math. Gen. 19 (1986) 423-435. Printed in Great Britain

The (2+1)D Ising model on a triangular lattice

C J Hamer† and C H J Johnson‡

† Department of Theoretical Physics, Research School of Physical Sciences, The Australian National University, Canberra, ACT 2601, Australia

‡ CSIRO Division of Chemical Physics, Clayton, Victoria 3168, Australia

Received 13 May 1985

Abstract. The (2+1)D Ising model on a triangular lattice is explored for lattices of up to 5×5 sites. Finite-size scaling techniques are used to estimate the critical parameters $x_c = 0.2096(2)$, $\nu = 0.627(4)$, $\beta = 0.322(6)$, $\gamma = 1.236(8)$. These agree with previous estimates, within errors, and with the hypotheses of universality and hyperscaling. The behaviour at low temperatures is also studied, and theoretical predictions of finite-size scaling at a first-order transition are confirmed.

1. Introduction

This paper is an extension of previous work (Hamer 1983, Henkel 1984) on finite-size scaling in the (2+1)D Ising model. We study a triangular rather than square lattice, and estimate magnetic as well as thermal critical indices. This enables a check of the universality between the square and triangular lattices; and furthermore, Privman (1983) has suggested that correction-to-scaling terms may be smaller for the magnetic indices on a triangular lattice, because of the higher coordination number.

The results obtained for the critical parameters are as follows: the critical coupling $x_c = 0.2096(2)$, and the critical indices $\nu = 0.627(4)$, $\beta = 0.322(7)$, $\gamma = 1.236(10)$. These indices agree within errors with other determinations, and confirm the expected universality between the square and triangular lattices, and between the (2+1)D and the more usual 3D formulations. The hyperscaling relation between the magnetic indices is also well satisfied. The only thorn in this rosy picture is the specific heat index α: no reliable result for this index can be obtained.

There have been several discussions in recent years of the finite-size scaling behaviour expected at a first-order transition (Blöte and Nightingale 1982, Privman and Fisher 1983). To study this question, we look at the low-temperature region of the model. The finite-lattice susceptibility is found to diverge (and the mass gap to decrease) exponentially with the area of the lattice, as predicted theoretically. Estimates of the interfacial tension can be deduced therefrom. Widom's (1974) scaling relation $\mu/\nu = 2$ is shown to follow naturally from the finite-size scaling hypotheses.

2. Finite-size scaling analysis

The Hamiltonian field theory version of the Ising model has been discussed by Fradkin and Susskind (1978), and see also Suzuki (1976). On a triangular spatial lattice of

0305-4470/86/030423+13$02.50

$M \times M$ sites, with a continuous time variable, the quantum Hamiltonian may be written

$$H = \frac{g}{2a}\left(\sum_m (1-\sigma_3(m)) - x \sum_{m,\hat{\mu}_i} \sigma_1(m)\sigma_1(m+\hat{\mu}_i) - h\sum_m \sigma_1(m)\right). \tag{2.1}$$

Here the index m labels sites on the spatial lattice, and the $\{\hat{\mu}_i\}$ are the three axis vectors of the triangular lattice. The σ_i are Pauli matrices acting on a two-state spin variable at each site, g is a dimensionless coupling constant (the 'temperature') and $x = 2/g^2$, a is the lattice spacing and h is the magnetic field. It is most convenient to work with the reduced Hamiltonian:

$$W \equiv \frac{2a}{g}H = M^2 - \sum_m \sigma_3(m) - x \sum_{m,\hat{\mu}_i} \sigma_1(m)\sigma_1(m+\hat{\mu}_i) - h\sum_m \sigma_1(m). \tag{2.2}$$

Periodic boundary conditions are assumed:

$$\sigma_1(m + M\hat{\mu}_i) = \sigma_1(m). \tag{2.3}$$

The correspondences between Hamiltonian field theory and statistical mechanics are by now well known (Kogut 1979, Barber 1984). If we denote the first two eigenvectors of the operator W as $|0\rangle$ and $|1\rangle$ respectively, and their eigenvalues by ω_0 and ω_1, the quantities of interest to us are the mass gap

$$F(x) = \omega_1(x) - \omega_0(x), \tag{2.4}$$

the Callan-Symanzik beta function

$$\beta(g)/g = F(x)/(F(x) - 2xF'(x)), \tag{2.5}$$

the 'specific heat' per site

$$\tilde{C}(x) = -(x^2/M^2)\,\partial^2\omega_0/\partial x^2, \tag{2.6}$$

and the susceptibility per site

$$\chi(x) = -(1/M^2)\,\partial^2\omega_0/\partial h^2|_{h=0}. \tag{2.7}$$

The spontaneous magnetisation is strictly zero for any finite lattice: but a finite-lattice observable can be found which converges smoothly to the spontaneous magnetisation in the bulk limit (Yang 1952, Uzelac 1980, Hamer 1982), namely

$$\mathcal{M}(x) = (1/M^2)\left\langle 1 \left| \sum_m \sigma_1(m) \right| 0 \right\rangle. \tag{2.8}$$

These quantities have been calculated for a sequence of different lattice sizes, $M = 1, 2, \ldots, 5$ (for details see the appendix), and finite-size scaling methods will be used to estimate their behaviour in the bulk limit, $M \to \infty$.

2.1. *High-temperature behaviour*

Well away from the critical point, the eigenvalues are expected to converge linearly to their bulk limit, and so an iterated Aitken algorithm can be used to estimate the bulk result from the finite-lattice values (Hamer and Barber 1981b). The results for the thermodynamic quantities of interest are illustrated in figures 1-3.

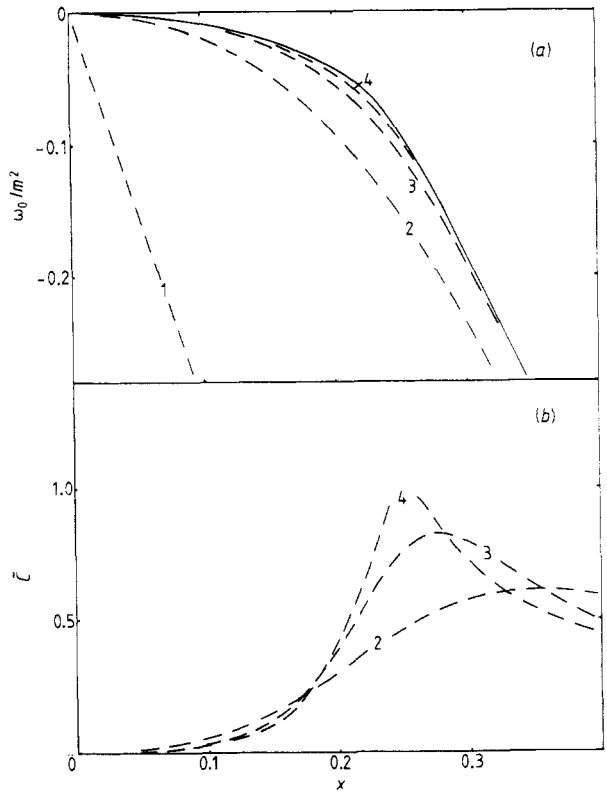

Figure 1. (*a*) Ground-state energy per site, and (*b*) specific heat per site, as functions of x. The broken curves are finite-lattice results, labelled by the lattice size M. The full curve is the estimated bulk limit, accurate to the order of the width of the curve, except where breaks occur.

For the beta function, the upper set of finite-lattice curves are the estimates (2.5) (Hamer *et al* 1978); the lower set are the Roomany-Wyld (1980) estimates,

$$\frac{\beta(g)}{g}=\frac{\ln(R_M(x))}{\ln[M/(M-1)]}\left(1-x\frac{\mathrm{d}}{\mathrm{d}x}\ln(F_M(x)F_{M-1}(x))\right)^{-1} \tag{2.9}$$

where $F_M(x)$ is the mass gap for lattice size M, and $R_M(x)$ is the 'scaled mass gap ratio'

$$R_M(x)=MF_M(x)/(M-1)F_{M-1}(x). \tag{2.10}$$

As usual, the Roomany-Wyld estimates converge remarkably quickly to the bulk limit.

It is also noteworthy that whereas the other observables display the expected rapid, linear convergence to the bulk limit in the high-temperature (small x) region, the 'magnetisation' $\mathcal{M}(x)$ is an exception to the rule, and converges 'logarithmically' (i.e. like a power of M) to its zero limiting value. This phenomenon will be discussed further in § 2.3.

A critical point at $x_c \simeq 0.21$ is clearly evident in all these data. The mass gap, beta function and magnetisation vanish there, while the specific heat and susceptibility show evidence of a divergence. The finite-lattice susceptibility in fact diverges strongly in the whole low-temperature region $x \geqslant x_c$: this will also be discussed in § 2.3.

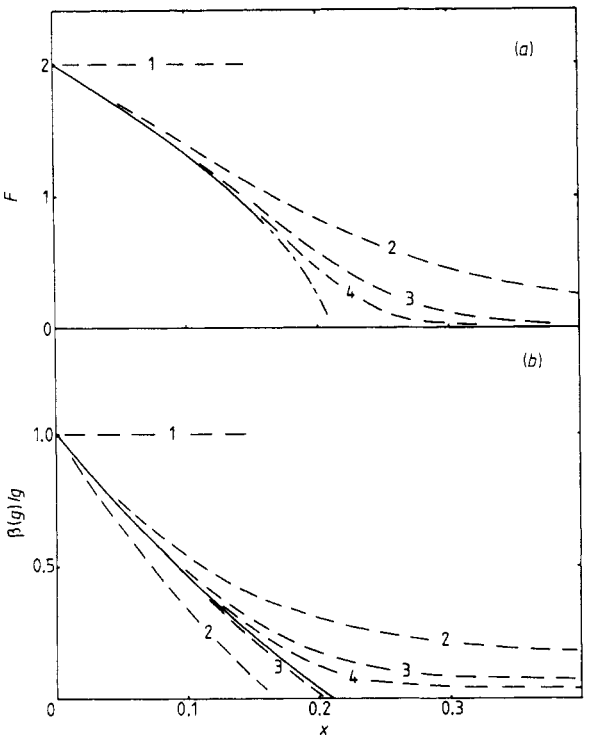

Figure 2. (*a*) The mass gap, and (*b*) the beta function, as a function of x. Conventions as in figure 1. In (*b*) the upper curves correspond to equation (2.5), the lower ones to the Roomany-Wyld estimates (2.9). The Roomany-Wyld estimate for $M = 4$ is indistinguishable from the bulk limit, and has been omitted.

2.2. Critical parameters

Finite-size scaling techniques can now be used to estimate the critical parameters (Nightingale 1976, Hamer and Barber 1981a, b). Firstly, a sequence of estimates of the critical point, $\{x_M\}$, can be found as solutions of the equation

$$R_M(x_M) = 1. \tag{2.11}$$

The results are listed in table 1. This sequence is expected to converge logarithmically, and Lubkin's algorithm (Lubkin 1952, Barber and Hamer 1982) has been used to estimate the bulk limit, giving

$$x_c = 0.2096 \pm 0.0002. \tag{2.12}$$

The exponent ν can be calculated from the finite-lattice beta function (2.5), whose scaling behaviour is

$$\beta_M(x_M) \underset{M\to\infty}{\sim} M^{-1/\nu}, \tag{2.13}$$

at the pseudo-critical points x_M. Hence one can use the estimate

$$\rho_M \equiv M\left(1 - \frac{\beta_M(x_M)}{\beta_{M-1}(x_M)}\right) \underset{M\to\infty}{\sim} \frac{1}{\nu}, \tag{2.14}$$

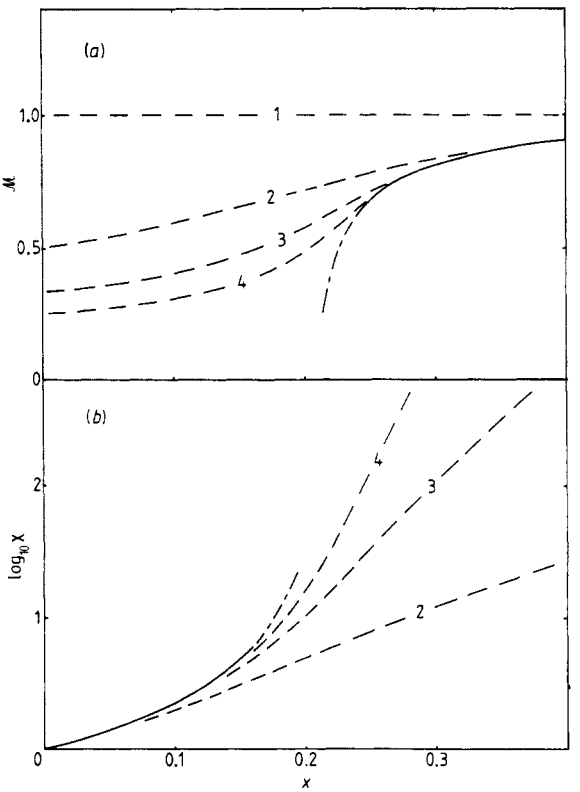

Figure 3. (*a*) The magnetisation, and (*b*) the susceptibility per site, as functions of x. Conventions as in figure 1.

or else a second estimate is

$$\tilde{\rho}_M \equiv -\frac{\ln[\beta_M(x_M)/\beta_{M-1}(x_M)]}{\ln[M/(M-1)]} \underset{M\to\infty}{\sim} \frac{1}{\nu}. \tag{2.15}$$

Both these sequences are displayed in table 1. It is worth noting that the results are almost identical with those obtained for the square lattice (Hamer 1983). The correction-to-scaling terms are smaller for the second, logarithmic sequence.

Table 1. Finite-size scaling estimates for the critical point x_c, and critical indices $1/\nu$ and α/ν, as defined by equations (2.11), (2.14), (2.15) and (2.18) of the text. M is the larger of the two lattice sizes used in each estimate. Also listed are the estimated bulk limits for each finite-lattice sequence, and the end shift ε at which this estimate was taken.

M	x_M	ρ_M	$\tilde{\rho}_M$	σ_M
2	0.166 699	1.283 79	1.481 54	2.0000
3	0.204 323	1.380 76	1.520 85	0.7676
4	0.208 169	1.432 57	1.541 24	0.5937
5	0.209 059	1.464 13	1.552 71	0.5191
Extrapolated value:	0.2096 (2)	1.60 (2)	1.594 (10)	0.34 (5)
ε:	0	0.48	0.12	−1.72

We now want to estimate the limit point of these sequences, which is a difficult and rather subjective business with sequences as short as this (Hamer 1983, Henkel 1984). We have applied both Aitken's algorithm and Lubkin's algorithm to extrapolate each sequence; and to test the stability and accuracy of the result, we have also applied an 'end-shift' $M \to M + \varepsilon$ in (2.14) and (2.15), where ε is a free parameter which does not affect the limit of the sequence (Hamer and Barber 1981b). A useful criterion appears to be to adjust ε so that the results of the Aitken and Lubkin extrapolations agree†. The results are shown in table 1. The sequence (2.15) leads to the more accurate estimate:

$$1/\nu = 1.594 \pm 0.01. \tag{2.16}$$

The ratio α/ν can be extracted from the finite-size scaling behaviour of the specific heat:

$$\tilde{C}_M(x_M) \underset{M\to\infty}{\sim} M^{\alpha/\nu} \tag{2.17}$$

whence

$$\sigma_M = M\left(1 - \frac{\tilde{C}_{M-1}(x_M)}{\tilde{C}_M(x_M)}\right) \underset{M\to\infty}{\sim} \frac{\alpha}{\nu}. \tag{2.18}$$

This sequence is also listed in table 1, and can be extrapolated to give an estimate

$$\alpha/\nu = 0.34 \pm 0.05. \tag{2.19}$$

The results are again similar to those obtained in the square lattice case (Hamer 1983), and the accuracy is equally poor in both cases. This appears to be due to the slow decrease of the correction-to-scaling terms for α/ν (Hamer and Barber 1981b).

The 'magnetisation' is associated with the ratio β/ν:

$$\mathcal{M}_M(x_M) \underset{M\to\infty}{\sim} M^{-\beta/\nu}. \tag{2.20}$$

The most rapidly convergent sequence of estimates is again the logarithmic one:

$$\tilde{\tau}_M \equiv -\frac{\ln[\mathcal{M}_M(x_M)/\mathcal{M}_{M-1}(x_M)]}{\ln[M/(M-1)]} \underset{M\to\infty}{\sim} \frac{\beta}{\nu} \tag{2.21}$$

which is shown in table 2. The correction-to-scaling terms are indeed very small for

Table 2. Finite-size scaling estimates for the critical indices β/ν and γ/ν, as defined by equations (2.21), (2.24) and (2.25) of the text. The estimated bulk limits and corresponding values of the end shift ε are also listed.

M	$\tilde{\tau}_M$	ϕ_M	$\tilde{\phi}_M$
2	0.566 713	5.295 88	1.867 08
3	0.514 431	3.676 50	1.973 00
4	0.512 813	3.061 81	1.975 82
5		2.767 50	1.974 11
Extrapolated value:	0.513 (10)	2.02 (10)	1.970 (5)
ε:		−1.36	−0.01

† The finite-lattice sequences near the critical point are expected to converge logarithmically, in which case the Lubkin algorithm is more suitable than Aitken's: and indeed the Lubkin result is more stable to the end shift ε.

this case, as predicted by Privman (1983); but unfortunately, we have been unable for technical reasons (see the appendix) to compute a value for $M = 5$, so the sequence is very short, and its extrapolation gives only

$$\beta/\nu = 0.513 \pm 0.01. \tag{2.22}$$

The finite-lattice susceptibility gives the ratio γ/ν:

$$\chi_M(x_M) \underset{M\to\infty}{\sim} M^{\gamma/\nu} \tag{2.23}$$

via the sequences

$$\phi_M \equiv M\left(\frac{\chi_M(x_M)}{\chi_{M-1}(x_M)} - 1\right) \underset{M\to\infty}{\sim} \frac{\gamma}{\nu} \tag{2.24}$$

and

$$\tilde{\phi}_M \equiv \frac{\ln[\chi_M(x_M)/\chi_{M-1}(x_M)]}{\ln[M/(M-1)]} \underset{M\to\infty}{\sim} \frac{\gamma}{\nu}. \tag{2.25}$$

These sequences are listed in table 2. Again, the correction-to-scaling terms appear least for the logarithmic sequence, and our best estimate is

$$\gamma/\nu = 1.970 \pm 0.005. \tag{2.26}$$

2.3. Low-temperature behaviour

The 'low-temperature' region $x > x_c$, $h = 0$, is a first-order transition line. A comprehensive discussion of the finite-size scaling behaviour expected at first-order transitions has been given recently by Privman and Fisher (1983). The basic features may be seen if we restrict ourselves to the subspace spanned by the two lowest eigenvectors $|0\rangle$ and $|1\rangle$, whose eigenvalues become degenerate in the bulk limit. For any finite lattice, the crossing between these two eigenvalues at $h = 0$ is 'avoided', as shown in figure 4(*a*). The reduced Hamiltonian W can be parametrised as

$$W = \begin{pmatrix} \omega_0 & h\alpha \\ h\alpha & \omega_0 + \delta \end{pmatrix} \tag{2.27}$$

for an $M \times M$ lattice with h small. Here

$$\omega_0/M^2 = f_0 - \tfrac{1}{2}h^2\chi_\infty + O(h^4) \tag{2.28}$$

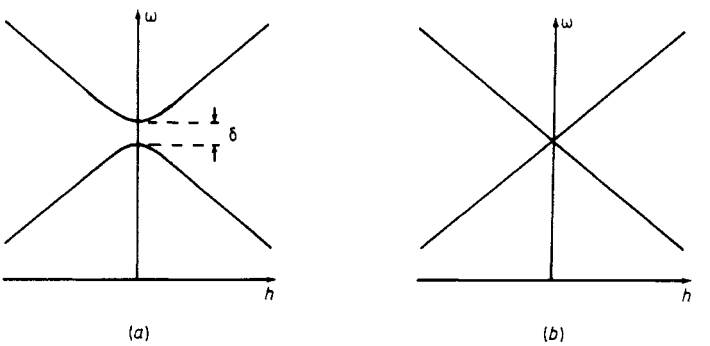

Figure 4. Structure of the lowest two Hamiltonian eigenvalues as a function of magnetic field h in the low-temperature region. (*a*) Finite-lattice case: 'avoided crossing', with mass gap δ. (*b*) Infinite-lattice case: degeneracy at $h = 0$.

where f_0 is the ground-state energy per site in the bulk (at $h=0$), and χ_∞ is the bulk susceptibility (which is relatively small, and will be ignored henceforth). The quantity δ is just the finite-lattice mass gap at $h=0$, and in the low-temperature region it is expected to vanish exponentially with the area of the lattice (Blöte and Nightingale 1982, Privman and Fisher 1983):

$$\delta \equiv F_M \underset{M\to\infty}{\sim} \tilde{D}(M)\exp(-M^2\bar{\sigma}) \qquad \text{for } x > x_c, \tag{2.29}$$

where $\bar{\sigma}$ is the reduced interfacial tension. Physically, this is because the splitting between the two eigenvalues is proportional to the transition amplitude between 'spin-up' and 'spin-down' magnetised states on the lattice. In the Euclidean framework, such a transition is suppressed by a Boltzmann factor involving the excess free energy associated with the interface† between the oppositely magnetised regions: this Boltzmann factor is just the exponential term in (2.29).

The linearised magnetic interaction term $h\alpha$ in (2.27) is related to the spontaneous magnetisation. In the bulk limit, as $\delta \to 0$, the slope of the eigenvalues at $h=0$ is equal to α (figure 4(b)), and so we find the spontaneous magnetisation is given by

$$\mathcal{M}_\infty = \lim_{\substack{M\to\infty \\ h\to 0}} \left(\frac{1}{M^2}\frac{\partial E_0}{\partial h} \right) = \frac{\alpha}{M^2}. \tag{2.30}$$

The quantity α/M^2 is just the matrix element used to estimate the magnetisation in equation (2.8).

Now the lowest eigenvalue of the matrix (2.27) is

$$\omega = \omega_0 + \delta/2 - (\delta^2/4 + h^2\alpha^2)^{1/2} \tag{2.31}$$

so that the *finite-lattice* susceptibility is

$$\chi_M = -\frac{1}{M^2}\frac{\partial^2\omega}{\partial h^2}\bigg|_{h=0} = \frac{2}{M^2}\frac{\alpha^2}{\delta} \underset{M\to\infty}{\sim} 2M^2\mathcal{M}_\infty^2\tilde{D}^{-1}(M)\exp(M^2\bar{\sigma}). \tag{2.32}$$

Thus the curvature at $h=0$ is extremely large, as shown in figure 4(a), building up to a δ-function singularity and a discontinuous change in slope in the bulk limit as in figure 4(b).

Let us now demonstrate this behaviour numerically. The rapid divergence of the finite-lattice susceptibility was already exhibited in figure 3(b). The equally rapid decrease of the mass gap is shown in figure 5(a), where a graph of $\log F_M$ against M^2 clearly shows a linear decrease. This can be used to estimate the interfacial tension, using the formula

$$\bar{\sigma}_M \equiv -\frac{\ln[F_M(x)/F_{M-1}(x)]}{2M-1} \underset{M\to\infty}{\sim} \bar{\sigma}(x) \tag{2.33}$$

which follows from (2.29). The results are shown in figure 5(b). It can be seen that the interfacial tension drops away towards zero at the critical point x_c. At larger x, it can be approximately fitted by a form

$$\bar{\sigma} \simeq 1.66(x-0.3)^{1/2}. \tag{2.34}$$

† The Hamiltonian formulation corresponds to a 'cylindrical geometry' in the language of Privman and Fisher (1983), in which the most likely interface runs across the cylinder, i.e. across the area of the spatial lattice, with the time direction corresponding to the longitudinal axis.

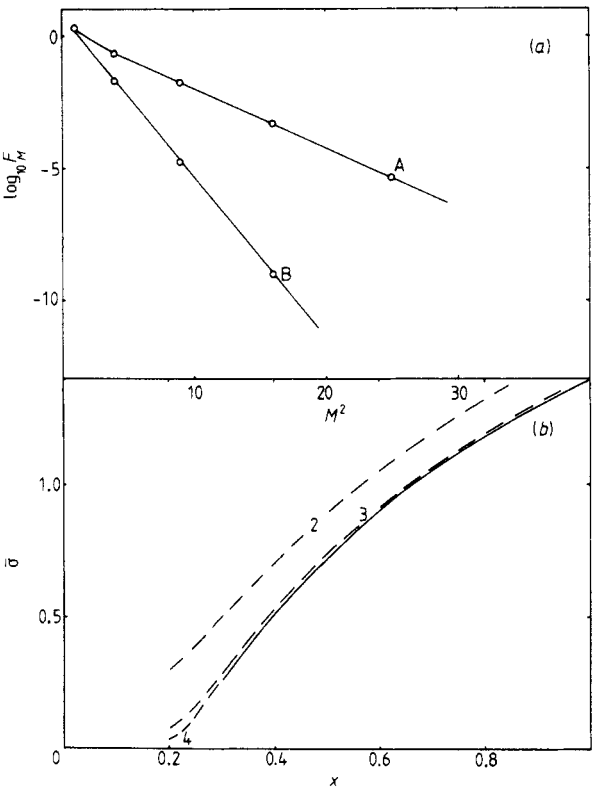

Figure 5. (*a*) The logarithm of the finite-lattice mass gap as a function of M^2, the area of the lattice. *A*, $x = 0.4$; *B*, $x = 1.0$. (*b*) The reduced interfacial tension as a function of x. Conventions as in figure 1.

2.4. Hyperscaling

The hypotheses of finite-size scaling theory, if consistently applied, imply many (if not all) of the hyperscaling relations. This is only to be expected, since the finite-size scaling behaviour can be derived from a renormalisation group analysis which itself implies hyperscaling (see, e.g., the review by Barber (1984)). Two examples can be extracted from the discussion above.

Firstly, one would expect the finite-lattice interfacial tension near the critical point to give the ratio μ/ν:

$$\bar{\sigma}_M(x_M) \underset{M\to\infty}{\sim} M^{-\mu/\nu}. \tag{2.35}$$

But then the definitions (2.33) or (2.29), together with the assumed scaling behaviour of the mass gap,

$$F_M(x_M) \underset{M\to\infty}{\sim} M^{-1} \tag{2.36}$$

necessarily imply Widom's (1974) scaling relation

$$\mu/\nu = 2. \tag{2.37}$$

Secondly, from equations (2.29) and (2.32) it follows that one can find another estimate of the spontaneous magnetisation as

$$\tilde{\mathcal{M}}_M \equiv (F_M \chi_M / M^2)^{1/2} \underset{M\to\infty}{\sim} \mathcal{M}_\infty. \tag{2.38}$$

The results are in fact almost identical (within 1 part in 10^5) to those shown in figure 3(a), corresponding to the definition (2.8). But then the usual finite-size scaling hypotheses for $\tilde{\mathcal{M}}_M$, F_M and χ_M near the critical point imply the hyperscaling relation

$$\gamma/\nu + 2\beta/\nu = 3. \tag{2.39}$$

This is indeed satisfied very nicely by the estimates (2.22) and (2.26). We note in passing that equation (2.38) explains the peculiar behaviour of the finite-lattice magnetisation in the high-temperature region: while F_M and χ_M converge in a rapid, linear fashion to their finite bulk limits, the magnetisation $\tilde{\mathcal{M}}_M$ (or $\mathcal{M}_M$) only converges to zero like $1/M$.

There have been persistent suggestions that hyperscaling is violated in the 3D Ising model (Freedman and Baker 1982). Binder *et al* (1985) discussed finite-size tests of hyperscaling in a recent paper, where the form of violation considered was due to a 'dangerous irrelevant variable'. It appears that in this case the 'effective' exponents extracted from a finite-size scaling analysis such as ours would still obey hyperscaling relations such as (2.39) but would no longer be equal to the *true* critical exponents. There is no way that this possibility can be tested within our present analysis.

3. Discussion

To summarise, our principal results for the critical parameters of the (2+1)D Ising model on a triangular lattice are

$$x_c = 0.2096(2), \tag{3.1}$$

$$1/\nu = 1.594(10), \qquad \text{hence } \nu = 0.627(4), \tag{3.2}$$

$$\beta/\nu = 0.513(10), \qquad \text{hence } \beta = 0.322(6), \tag{3.3}$$

$$\gamma/\nu = 1.970(5), \qquad \text{hence } \gamma = 1.236(8). \tag{3.4}$$

These were obtained from a sequence of triangular $M \times M$ lattices up to $M = 5$ sites. High-temperature series results for the same model are (Hamer and Irving 1984):

$$x_c = 0.209\,76(15), \qquad \gamma = 1.247(5), \qquad \nu = 0.64(2), \tag{3.5}$$

and from a low-temperature series analysis (Marland 1981)

$$x_c = 0.2098(2), \qquad \gamma' = 1.250(12), \qquad \beta = 0.315(2), \qquad \alpha' = 0.098(3). \tag{3.6}$$

These values agree with ours within errors, except in the case of the specific heat index α. As explained in the previous section, we place little reliance on our determination of this quantity.

Finite-size scaling results for the (2+1)D Ising model on a square lattice were $\nu = 0.635(5)$ (Hamer 1983), and $\nu = 0.629(2)$, $\beta = 0.324(9)$ (Henkel 1984). These agree with our present results (3.2) and (3.4).

The most accurate recent estimates for the 3D Ising model are

$$\nu = 0.629(2), \qquad \gamma = 1.238(3), \qquad \alpha = 0.12(2) \tag{3.7}$$

from high-temperature series analyses on the BCC lattice (Adler *et al* 1982, Ferer and Velgakis 1983, Adler 1983);

$$\nu = 0.630(2), \qquad \gamma = 1.241(2), \qquad \beta = 0.325(2), \qquad \alpha = 0.110(5), \tag{3.8}$$

from field-theory methods (Le Guillou and Zinn-Justin 1980, Baker *et al* 1978);

$$\nu = 0.629(4) \tag{3.9}$$

from a Monte Carlo renormalisation group calculation (Pawley *et al* 1984); and $\gamma/\nu = 1.98 \pm 0.02$ from a Monte Carlo finite-size scaling analysis (Barber *et al* 1984).

It appears that, except in the case of the index α, our results agree within errors with other determinations. The expected universality between the square and triangular lattices, and between the (2+1)D model and the 3D model, is thus confirmed.

Our accuracy is somewhat less than that obtained by other methods†, but nevertheless it is useful to confirm these other results by a different approach. To improve the accuracy substantially, one must obtain eigenvalues for a 6×6 lattice: this system is much too large to analyse exactly (Hamer 1983), but it might be possible to obtain sufficiently precise eigenvalues by some approximation technique.

We have also studied the behaviour of the triangular lattice system in the low-temperature region. The predicted exponential decrease of the finite-lattice mass gap with area (Blöte and Nightingale 1982, Privman and Fisher 1983) has been confirmed, and has been used to extract values for the 'reduced interfacial tension' in this model.

Finally, a brief discussion of hyperscaling was given. It was shown that the hypotheses of finite-size scaling imply relations such as

$$\mu/\nu = 2 \tag{3.10}$$

and

$$\gamma/\nu + 2\beta/\nu = 3 \tag{3.11}$$

and indeed our results (3.3) and (3.4) satisfy the latter relation to within 0.2%. A third hyperscaling relation,

$$2/\nu - \alpha/\nu = 3, \tag{3.12}$$

is not satisfied, but this is most likely due to our poor value for α/ν.

Acknowledgments

This investigation was made possible by a CSIRO/ANU Collaborative Research Grant, for which we record our gratitude. We would also like to thank Drs V Privman and M Henkel for valuable correspondence. Finally, we would like to thank the staff of CSIRONET, especially Drs P Price and G Havas, and Jan Bubb, for their help in getting our programs to run.

Appendix. Numerical methods

The calculations described in this paper were carried out on a CYBER 205 computer, and occupied approximately 75 min CPU time. The Hamiltonian matrix for the 5×5

† Although note that the value $\gamma/\nu = 1.970(6)$ obtained from the field-theory values (3.8) is of about the same accuracy as our (3.4), and agrees with it exactly.

lattice involved 115 904 basis states, and approximately 5.5×10^6 non-zero matrix elements.

The 205 is a vector processing machine, which operates most efficiently when processing a long string of contiguous data elements in memory. We have endeavoured to adapt previous numerical techniques (Roomany *et al* 1980, Irving and Thomas 1982, Hamer 1983) to this situation as follows.

(i) In the first stage of the calculations, which is the generation of the Hamiltonian matrix, the 'core' routine occupying most of the CPU time is that which transforms a given spin configuration by translations, rotations and reflections to find the 'minimum' representative configuration, and its symmetry factor under these transformations. For each 'up' spin in the original configuration, represented by a 'set' bit in the spin vector, the corresponding contribution to each transformed configuration can be given as an additive binary number, 2^n, where n is the position of that spin in the transformed configuration. Thus all of the $12 \times 25 = 300$ transformed configurations can be found by 25 vector additions, each involving 300 contiguous elements.

(ii) In the second stage of the calculation, which is the calculation of the matrix eigenvalues by a Lanczos algorithm, it is not so easy to 'vectorise' the calculations. The 'core' routine involves the multiplication of the Hamiltonian matrix into a given state vector: but since the matrix is sparse, there is no natural structure involving contiguous data elements. The best we have been able to do is to treat 15 or 20 different parameter values at once, and 'vectorise' the multiplications in these parameters. To minimise page faults, the Hamiltonian matrix was broken up into 'blocks', so that only a restricted subset of the basis state amplitudes were needed at any one time.

The Lanczos routine used in these calculations provided an accurate estimate of the ground-state eigenvalue, but no accompanying eigenvector: hence we were unable to calculate the finite-lattice magnetisation for the 5×5 lattice. Henkel (1984) used a two-step iterative Lanczos algorithm which does provide a reliable eigenvector.

References

Adler J 1983 *J. Phys. A: Math. Gen.* **16** 3585

Adler J, Moshe M and Privman V 1982 *Phys. Rev.* B **26** 3958

Baker G, Nickel B G and Meiron D I 1978 *Phys. Rev.* B **17** 1365

Barber M N 1984 *Phase Transitions and Critical Phenomena* vol 8, ed C Domb and J L Lebowitz (New York: Academic) pp 146–268

Barber M N and Hamer C J 1982 *J. Aust. Math. Soc.* B **23** 229

Barber M N, Pearson R B, Toussaint D and Richardson J L 1985 *Phys. Rev.* B **32** 1720

Binder K, Nauenberg M, Privman V and Young A P 1985 *Phys. Rev.* B **31** 1498

Blöte H W J and Nightingale M P 1982 *Physica* **112A** 405

Ferer M and Velgakis M J 1983 *Phys. Rev.* B **27** 2839

Fisher M E 1974 *Renormalization Group in Critical Phenomena and Quantum Field Theory* ed J D Gunton and M S Green (Philadelphia: Temple University Press)

Fradkin E and Susskind L 1978 *Phys. Rev.* D **17** 2637

Freedman B A and Baker G A 1982 *J. Phys. A: Math. Gen.* **15** L715

Hamer C J 1982 *J. Phys. A: Math. Gen.* **15** L675

—— 1983 *J. Phys. A: Math. Gen.* **16** 1257

Hamer C J and Barber M N 1981a *J. Phys. A: Math. Gen.* **14** 241

—— 1981b *J. Phys. A: Math. Gen.* **14** 2009

Hamer C J and Irving A C 1984 *J. Phys. A: Math. Gen.* **17** 1649

Hamer C J, Kogut J B and Susskind L 1978 *Phys. Rev. Lett.* **41** 1337

Henkel M 1984 *J. Phys. A: Math. Gen.* **17** L795

Irving A C and Thomas A 1982 *Nucl. Phys.* B **200** 424
Kogut J 1979 *Rev. Mod. Phys.* **51** 659
Le Guillou J C and Zinn-Justin J 1980 *Phys. Rev.* B **21** 3976
Lubkin S 1952 *J. Res. NBS* **48** 228
Marland L G 1981 *J. Phys. A: Math. Gen.* **14** 2047
Nightingale M P 1976 *Physica* A **83** 561
Pawley G S, Swendson R H, Wallace D J and Wilson K G 1984 *Phys. Rev.* B **29** 4030
Privman V 1983 Private communication
Privman V and Fisher M E 1983 *J. Stat. Phys.* **33** 385
Roomany H and Wyld H W 1980 *Phys. Rev.* D **21** 3341
Roomany H, Wyld H W and Holloway L E 1980 *Phys. Rev.* D **21** 1557
Suzuki M 1976 *Prog. Theor. Phys.* **56** 1454
Uzelac K 1980 *Thesis* Orsay
Widom B 1974 *Phase Transitions and Critical Phenomena* vol 2, ed C Domb and M S Green (New York: Academic) pp 79-100
Yang C N 1952 *Phys. Rev.* **85** 808